HHS Public Access

Author manuscript

J Cyst Fibros. Author manuscript; available in PMC 2018 March 01.

Published in final edited form as:

J Cyst Fibros. 2017 March ; 16(2): 283–290. doi:10.1016/j.jcf.2015.11.009.

Preliminary Comparison of Normalized T1 and Non-Contrast Perfusion MRI Assessments of Regional Lung Disease in Cystic Fibrosis Patients

Shannon B. Donnola[1], **Elliott C. Dasenbrook**[2,3,4], **David Weaver**[2,4], **Lan Lu**[1,5], **Karishma Gupta**[1], **Anjali Prabhakaran**[6], **Xin Yu**[1,7,8], **James F. Chmiel**[2,4], **Kimberly McBennett**[2,3,4], **Michael W. Konstan**[2,4], **Mitchell L. Drumm**[2,9], and **Chris A. Flask**[1,2,7,*]

[1]Department of Radiology, Case Western Reserve University, Cleveland, Ohio, United States of America

[2]Department of Pediatrics, Case Western Reserve University, Cleveland, Ohio, United States of America

[3]Department of Medicine, Case Western Reserve University, Cleveland, Ohio, United States of America

[4]Rainbow Babies and Children's Hospital, Cleveland, Ohio, United States of America

[5]Department of Urology, Case Western Reserve University, Cleveland, Ohio, United States of America

[6]Lake Ridge Academy, North Ridgeville, Ohio, United States of America

[7]Department of Biomedical Engineering, Case Western Reserve University, Cleveland, Ohio, United States of America

[8]Department of Physiology and Biophysics, Case Western Reserve University, Cleveland, Ohio, United States of America

[9]Department of Genetics, Case Western Reserve University, Cleveland, Ohio, United States of America

Keywords

Magnetic Resonance Imaging; imaging; perfusion; relaxometry; lung disease

[*]Corresponding author: Chris A. Flask, PhD, Associate Professor of Radiology, 11100 Euclid Ave/Bolwell B115, Cleveland, OH 44106, 216-844-4963, caf@case.edu.

INTRODUCTION

The leading cause of shortened survival in cystic fibrosis (CF) is progressive lung disease associated with recurrent pulmonary infections.[1,2] An essential component for the clinical management of patients with CF is the capability to longitudinally monitor the progression of lung disease and therapeutic efficacy. Unfortunately, current clinical assessments of CF lung disease are either invasive (bronchoalveolar lavage, BAL [3,4]), expose patients to significant repeated doses of ionizing radiation (X-ray and/or Computed Tomography (CT)) [5–7], or offer limited sensitivity to detect early-stage, regional lung disease (spirometry). Therefore, the development of a sensitive, non-invasive, and radiation-free method for assessing CF lung disease is the essential next step towards improving health care for patients with CF.[8]

Magnetic Resonance Imaging (MRI) is a safe, non-invasive technique that can provide quantitative assessments of lung disease without ionizing radiation (as for X-ray and CT). [9–14] Multiple recent reports suggest that MRI can be used to detect and quantify lung disease in patients with CF.[12,15–20] Hyperpolarized (HP) MRI techniques have also been shown to detect changes in lung structure/function.[10,21,22] Unfortunately, these HP MRI techniques require specialized equipment and inhaled contrast agents and are therefore only available on a limited number of MRI scanners. Thanks to advances in MRI hardware and acquisitions, conventional proton MRI techniques can now be used to assess lung structure and function non-invasively without ionizing radiation or injectable contrast agents. For example, our team has recently developed a normalized T1 (nT1) MRI technique to rapidly (~5 seconds) detect early-stage lung disease in patients with CF despite no change in spirometry.[17] Other MRI studies have shown that pulmonary perfusion as measured by Arterial Spin Labeling (ASL) MRI is reduced in patients with CF compared to healthy control subjects and that this decrease in perfusion is associated with chronic lung disease and declining pulmonary function.[9,16] However, these promising quantitative MRI techniques have not been studied side by side in the same cohort of subjects with CF, and hence their sensitivity to detect CF lung disease has not been directly compared.

In this initial cross-sectional study, we obtained both normalized T_1 and pulmonary perfusion in 8 subjects with CF with a range of lung function (FEV_1 % predicted = 45 – 127%) compared to healthy control subjects (n = 6). The imaging data were obtained in a single MRI scanning session to ensure accurate image co-registration and the consistency of the pathophysiologic status for each subject. A lobe-by-lobe analysis of each subject's left and right lungs was performed to compare the sensitivity of each technique to detect regional changes in lung structure/function.

MATERIALS AND METHODS

Study Population

Eight adult cystic fibrosis patients with a range of pulmonary function were recruited from the CF center at University Hospitals/Rainbow Babies and Children's Hospital. All subjects with CF were scanned at baseline with no symptoms of acute pulmonary exacerbation. Spirometry assessments were obtained for each subject immediately prior to or following the

MRI scan. Young adult healthy volunteers with no prior history of chronic lung disease were recruited as controls from the student population at our institution. All MRI scans and spirometry assessments were performed according to approved Institutional Review Board (IRB) protocols.

Quantitative MRI Acquisitions

All subjects were scanned in a supine position using a Siemens Espree 1.5T MRI scanner (Siemens Medical Systems, Erlangen, Germany). To maximize image uniformity, spine array (posterior) and body array (anterior) coils were positioned over each subject's lungs. Initial localizer and proton density-weighted HASTE images (Half-Fourier Acquisition Single-shot Turbo spin Echo, respiratory triggered, TR/TE = 1000/24 ms, slice thickness = 15 mm, 10 slices, FOV = 400 mm × 400 mm, partial Fourier factor 5/8, 1 average) were first acquired to obtain the anatomic image of both the left and right lungs and to position the slices for the nT1 and ASL MRI acquisitions.

A rapid Look-Locker acquisition was used to generate dynamic T1-weighted images in order to calculate quantitative T1 maps of each subject's lungs [17] (TR/TE = 1.8 ms/0.84 ms, FOV= 400 mm × 400 mm, matrix size = 64 × 128, flip angle = 8°, slice thickness = 15mm, 40 images following the initial inversion). Prior to image reconstruction, the acquired imaging data were first zero padded to 128 × 128 matrix for isotropic resolution. Importantly, the Look-Locker acquisition was applied with a 5-second voluntary breath hold for each imaging slice to limit respiratory motion artifacts. The nT1 acquisition was repeated over 4–6 slices to enable a thorough sampling of each subject's left and right lungs. Absolute T1 relaxation time maps (in milliseconds) were calculated for each imaging slice using previously established models. [26] Normalized T1 maps were calculated by dividing the absolute T1 maps by the mean T1 value in the central region of each subject's lungs as described previously.[17]

The ASL MRI data for each subject were acquired using a ASL-FISP (ASL Fast Imaging with Steady-State Free Precession) method that combines a conventional flow-sensitive alternating inversion recover (FAIR) ASL preparation with a centrically-encoded FISP readout to limit image banding artifacts [23] (TR/TE = 3.0 ms/1.5 ms, FOV = 400 mm × 400 mm, matrix size = 128 × 128, flip angle = 60°, slice thickness = 15 mm). A hyperbolic recant adiabatic inversion pulse was used to ensure the uniformity of inversion pulse enabling accurate and precise quantification of tissue perfusion. The ASL data were obtained at the same sagittal imaging slices as for the nT1 assessments described above to accurately compare these MRI methods. The ASL acquisition included three sequential scans: 1) a flow-insensitive image acquired with a nonselective inversion pulse; 2) a flow-sensitive image acquired with a slice-selective inversion pulse, and 3) a reference image with no inversion preparation. The thickness of the slice selective inversion pulse was set to 45 mm (i.e., three times that of the imaging slice) to ensure uniform inversion over the imaging slice. A delay of 1.3 seconds was applied immediately following the inversion pulses. An additional 5-second delay was added between the ASL averages to allow the magnetization to fully relax back to equilibrium. Prospective and retrospective gating were also used to obtain multiple ASL signal averages (n=30) with minimal motion artifacts and a high signal-

to-noise ratio to enable accurate perfusion quantification. Quantitative ASL-based perfusion maps (in ml/min/100g of tissue) were calculated using established methods. [24,25]

Image and Statistical Analysis

All MRI images were exported for processing offline in Matlab (The Mathworks, Natick, MA). The sagittal normalized T1 (nT1) and perfusion (ASL) maps were analyzed by two separate raters to identify the individual lobes (left lung: upper and posterior; right lung: upper, anterior, and posterior). These regions-of-interest (ROIs) were then used to calculate mean nT1 and perfusion values in each lobe for each subject.

Two-tailed unpaired Student's t-tests were performed on the mean lobe-by-lobe imaging data to compare the imaging findings between the subjects with CF and healthy control subjects. Two-tailed unpaired Student's t-tests were also utilized to compare the results among different lobes within the CF and healthy control cohorts, respectively. In addition, mean nT1 and pulmonary perfusion values in the left (two) and right (three) lobes were plotted against spirometry results (FEV_1% predicted) for all subjects. Scatterplots of mean nT1 verses perfusion were also generated for each lobe for all subjects to determine the association between the MRI results. Pearson correlation coefficients (R) were determined for these analyses using a least squared error fit to a linear model. A p-value of less than 0.05 was considered statistically significant for the means comparisons and the correlations.

RESULTS

Study Population

A total of 8 subjects with CF and 6 healthy control subjects were enrolled in this study. Of the eight subjects with CF (5 male, 3 female; age = 18–49), four of them showed essentially normal lung function by spirometry (FEV_1 % predicted range = 91%–127%); three subjects were observed with mildly to moderately impaired lung function (FEV_1 % predicted range = 54%–79%) and one patient was found to have more severely impaired lung function (FEV_1 % predicted = 45%). The healthy control subjects (4 male, 2 female, age range = 18–45) had no prior history of lung disease or tobacco use, and had spirometry results within the normal range (FEV_1 % predicted range = 95% – 131%).

Example ROI's were drawn to delineate the upper (U) and posterior (P) lobes of the left lung as well as the upper (U), anterior (A), and posterior (P) lobes of the right lung (Figure 1). High resolution sagittal anatomic images (Figure 1, 1st column) were used as a guide to help distinguish the lobes in the nT1 and ASL-based perfusion maps for each subject. Figure 2 shows representative nT1 and ASL-based perfusion maps in the left and right lungs from a healthy control subject (top row) and a subject with CF lung disease (FEV_1 % predicted = 45%, bottom row). As expected, the nT1 and perfusion maps for the healthy control subject were relatively homogenous across the entire left and right lung. In contrast, the maps for the subject with CF showed visible decreases in nT1 and perfusion values, especially in the upper lobes.

The mean nT1 values in the lobes of the left lung (2 lobes) and right lung (3 lobes) were determined for each subject in order to compare the cohorts of CF subjects with healthy

control subjects (Fig. 3). Mean nT1 values for the subjects with CF were significantly reduced in comparison to healthy controls in the upper lobe of left lung (Fig. 3A, 0.859 vs. 0.977, p = 0.00008) as well as in the upper and anterior lobes of the right lung (Fig. 3B, 0.896 vs. 0.996, p = 0.0009; 0.888 vs. 0.993, p = 0.0002, respectively). Within the CF cohort, mean nT_1 values were significantly reduced in the upper lobe of the left lung (Fig. 3A, 0.894 vs. 0.9630, p = 0.0002) and upper and anterior lobes of the right lung (Fig. 3B, U vs. P, p = 0.0006; A vs. P lobe, p = 0.0005) in comparison to the respective left and right posterior lobes. Significantly lower mean perfusion values were also observed in the upper right lobe of CF subjects in comparison to the healthy controls (Fig. 4B, 968 vs. 1275 ml/min/100g of tissue, p=0.02). The perfusion assessments also demonstrated that the upper right lobes of the subjects with CF were significantly reduced compared to the perfusion in their right posterior lobes (968 vs. 1287 ml/min/100g of tissue, p=0.02) (Fig. 4B). No statistically significant differences in perfusion were observed in the left lungs.

Mean values for nT1 and pulmonary perfusion in the upper lobes plotted against the corresponding spirometry results for each subject are shown in Figure 5. The upper left lobe demonstrated a significant correlation between nT1 and spirometry (Fig. 5A, R = 0.68, p = 0.008). However, although there appears to be a trend, the right upper lobe's normalized T1 values were not significantly correlated with lung function assessments by spirometry (Fig. 5B, R = 0.46, p = 0.1). A significant correlation was observed between perfusion in the left and right upper lobes and spirometry (Fig. 5C, R = 0.55, p = 0.05; Fig. 5D, R = 0.64, p = 0.01). The anterior lobe in the right lung and posterior lobes of the left and right lungs were found to have no significant correlation with either nT1 or perfusion (data not shown).

The scatterplot comparing nT1 and perfusion for the upper left and right lobes of all subjects are shown in Figure 6. A significant correlation was observed between nT1 and perfusion in both the left and right upper lobes of patients with CF (Fig. 6A, R = 0.56, p = 0.05; Fig. 6B, R = 0.71, p = 0.005, respectively). No significant correlation was observed in any other lobes of the left and right lungs.

DISCUSSION

In this pilot study, we evaluated the sensitivity of the nT1 and ASL MRI techniques to detect lobular changes in subjects with CF compared to healthy control subjects. We found that both MRI methods were able to detect significant reductions in nT1 and pulmonary perfusion in regions of the left and right lungs for the cohort of subjects with CF compared to healthy control subjects (Figure 3). More specifically, the nT_1 results revealed significant decreases in the upper and anterior lobes of the right lungs as well in the upper lobe of the left lung for subjects with CF in comparison to healthy control subjects. Similar lobular reductions in nT1 were observed within the CF cohort in comparison to the posterior lobes. By comparison, the ASL-based perfusion results showed a significant decrease in pulmonary perfusion in the upper right lobes of the subjects with CF in comparison to healthy control subjects as well as between the upper and posterior lobes within the CF cohort (Figure 4). Overall, these initial cross-sectional imaging results suggest that both MRI metrics can detect and quantify regional lung disease in CF subjects. Importantly, these results suggest that nT1 may provide a more sensitive detection of regional lung disease in CF patients. It is

also important to note that these nT1 and perfusion changes were detected in the upper lobe of the right lungs of subjects with CF where CF lung disease is thought to often originate. [5]

The nT1 technique has some inherent advantages over the ASL-based perfusion methodology. As described previously, the nT1 normalization process limits the impact of individual anatomic variation in lung vasculature. [17] This reduction in variation improved the sensitivity of the nT1 methodology to detect early-stage lung disease in subjects with CF with essentially "normal" spirometry. In addition, the nT_1 data are acquired in a single ~5-second breath hold. Therefore, the nT1 technique provides an opportunity to effectively scan both lungs of young patients in as short as 5–10 minutes. In comparison, ASL techniques typically require multiple signal averages acquired over multiple breath-holds and/or breathing cycles (~5 minutes/imaging slice). In this implementation, the ASL images were acquired with both prospective and retrospective gating to acquire 30 averages to provide accurate quantification of pulmonary perfusion. As a result, the reduced variation provided by the nT1 methodology provided additional significant reductions in the anterior lobe of the right lung and the upper lobe of the left lung in subjects with CF in comparison to control subjects despite no statistical differences in perfusion (Figures 3 and 4). Improvements to the ASL methodology may provide the opportunity to acquire the perfusion data in a single breath-hold similar to the nT1 technique. [29] However, future studies will be needed to determine if improved ASL imaging strategies would then be capable of detecting reductions in the anterior lobes of patients with CF similar to the nT1 methodology.

While the nT1 assessment appears to be associated with pulmonary perfusion (Figure 6); the improved sensitivity of the nT1 technique to detect additional changes in the left and right lungs of CF patients may also be due in part to the specific (patho)physiologic features detected by these two MRI methods. As a methodology, ASL specifically detects the rate of pulmonary perfusion to the lungs and can be impacted by pulmonary blood volume, cardiac output, and regional vascular permeability. [13,26,27] On the other hand, the nT1 maps are largely reflective of blood volume independent of cardiac output. [17,28] While these subjects with CF were known to be at their usual baseline health status, it may be possible that the nT1 technique detected residual, sub-clinical edema in some subjects. Regardless, a larger cohort of subjects with CF will need to be studied in order to more thoroughly understand the differential pathophysiologic sensitivities of these two related, but complementary, imaging methodologies.

The nT1 and pulmonary perfusion results in the upper lobes of the left and right lungs were also compared to spirometry to determine if these imaging metrics correlated with pulmonary function. As shown in Figure 5, mean nT1 and perfusion in the upper lobe of the left lung both resulted in a significant correlation with spirometry. In contrast, only perfusion resulted in a significant correlation with spirometry in the upper right lobe. Prior published studies have also shown a significant correlation of nT1 with lung function in early-stage subjects with CF [17], suggesting that increasing the number of subjects with CF in this study will likely result in significant correlations for nT1 with lung function. Overall, these results are consistent with prior reports that both nT1 and perfusion MRI assessments are associated with declining pulmonary function in CF patients. [9,16, 17]

In general, the two MRI metrics described herein offer multiple advantages as a measure of CF lung disease. The MRI assessments are obtained non-invasively with no injectable contrast agent or ionizing radiation. These attributes make these imaging techniques inherently safe for longitudinal imaging assessments in both pediatric and adult patients with CF. In addition, this study demonstrates that these methods are sensitive to regional lung differences. Further, both of the clinically-viable MRI techniques are either already available (perfusion) or capable of being easily implemented (nT1) on virtually any modern MRI scanner. Therefore, these two MRI methods may provide safe, widely-available, and objective assessments for regional lung disease in CF patients.

A number of future studies must be conducted to further verify the utility of the nT1 and/or ASL MRI techniques for patients with CF. First, the CF cohorts must be expanded to include infant and young pediatric patients with early-stage lung disease. As described above, prior efforts suggest that nT1 can detect CF lung disease more sensitively than spirometry. However, few MRI studies have been conducted in infants with CF where emergent therapies will be most effective. In addition, each of these imaging techniques must also be evaluated in longitudinal imaging studies to i) establish the sensitivity of these methods to detect CF lung disease progression; and ii) determine the effect of acute pulmonary exacerbations on the imaging results. However, the preliminary results shown here suggest that nT1 and ASL MRI can provide a sensitive assessment of regional CF lung disease. Additional studies must be conducted to determine the association between these quantitative MRI assessments and other observable features of CF lung disease including bronchiectasis.

In conclusion, this initial study confirmed that both nT1 and ASL MRI can sensitively detect regional lung disease in patients with CF. However, additional nT1 reductions observed within the CF cohort suggest that nT1 may provide a more sensitive assessment of CF lung disease. Altogether, these results suggest that 1) nT1 and ASL can detect regional CF lung disease; 2) pulmonary perfusion and nT1 are significantly correlated with lung function; and 3) nT1 may be more sensitive than ASL-based perfusion to detect subtle CF lung disease. As these methods continue to be improved, our next goal is to gain a better understanding of the underlying pathophysiology of CF lung disease that will open new avenues for targeted therapeutics and early stage treatments that prevent irreversible lung damage in patients with CF.

Acknowledgments

The authors would like to acknowledge the support of The Cystic Fibrosis Foundation, NIH/NIDDK RO1 DK085099, NIH/NIDDK K12 DK100014, the Case Comprehensive Cancer Center (NIH/NCI P30 CA43703), and the Clinical and Translation Science Collaborative of Cleveland (NIH/NCATS UL1 TR000439). We would also like to acknowledge the support of Dr. Peter Jakob (University of Wurzburg) for his kindly assistance in providing the Look-Locker acquisition and image reconstruction algorithm.

References

1. Cystic fibrosis foundation, patient registry 2010 annual data report. Bethesda, MD: 2011.
2. Davis PB, Drumm M, Konstan MW. Cystic Fibrosis. Am J Resipiratoral Crit Care Med. 1996; 154:1229–56.

3. Wainwright CE, Vidmar S, Armstrong DS, Byrnes CA, Carlin JB, Cheney J, et al. Effect of bronchoalveolar lavage-directed therapy on Pseudomonas aeruginosa infection and structural lung injury in children with cystic fibrosis: a randomized trial. JAMA. 2011; 306:163–71. DOI: 10.1016/j.yped.2012.03.075 [PubMed: 21750293]

4. Belessis Y, Dixon B, Hawkins G, Pereira J, Peat J, MacDonald R, et al. Early cystic fibrosis lung disease detected by bronchoalveolar lavage and lung clearance index. Am J Respir Crit Care Med. 2012; 185:862–73. DOI: 10.1164/rccm.201109-1631OC [PubMed: 22323305]

5. Li Z, Sanders DB, Rock MJ, Kosorok MR, Collins J, Green CG, et al. Regional differences in the evolution of lung disease in children with cystic fibrosis. Pediatr Pulmonol. 2011; doi: 10.1002/ppul.21604

6. Brody AS, Tiddens HAWM, Castile RG, Coxson HO, De Jong PA, Goldin J, et al. Computed tomography in the evaluation of cystic fibrosis lung disease. Am J Respir Crit Care Med. 2005; 172:1246–52. DOI: 10.1164/rccm.200503-401PP [PubMed: 16100011]

7. Sanders DB, Li Z, Rock MJ, Brody AS, Farrell PM. The sensitivity of lung disease surrogates in detecting chest CT abnormalities in children with cystic fibrosis. Pediatr Pulmonol. 2012; 47:567–73. DOI: 10.1002/ppul.21621 [PubMed: 22170734]

8. Dasenbrook EC, Konstan MW. Inhaled hypertonic saline in infants and young children with cystic fibrosis. JAMA. 2012; 307:2316–7. DOI: 10.1001/jama.2012.5853 [PubMed: 22610477]

9. Schraml C, Schwenzer NF, Martirosian P, Boss A, Schick F, Schäfer S, et al. Non-invasive pulmonary perfusion assessment in young patients with cystic fibrosis using an arterial spin labeling MR technique at 1. 5 T. Magn Reson Mater Physics, Biol Med. 2012; 25:155–62. DOI: 10.1007/s10334-011-0271-x

10. Lipson DA, Roberts DA, Hansen-Flaschen J, Gentile TR, Jones G, Thompson A, et al. Pulmonary ventilation and perfusion scanning using hyperpolarized helium-3 MRI and arterial spin tagging in healthy normal subjects and in pulmonary embolism and orthotopic lung transplant patients. Magn Reson Med. 2002; 47:1073–6. DOI: 10.1002/mrm.10172 [PubMed: 12111953]

11. Ohno Y, Koyama H, Nogami M, Takenaka D, Matsumoto S, Obara M, et al. Dynamic oxygen-enhanced MRI versus quantitative CT: pulmonary functional loss assessment and clinical stage classification of smoking-related COPD. AJR Am J Roentgenol. 2008; 190doi: 10.2214/AJR.07.2511

12. Jakob PM, Wang T, Schultz G, Hebestreit H, Hebestreit A, Hahn D. Assessment of human pulmonary function using oxygen-enhanced T(1) imaging in patients with cystic fibrosis. Magn Reson Med. 2004; 51:1009–16. DOI: 10.1002/mrm.20051 [PubMed: 15122684]

13. Mai VM, Berr SS. MR perfusion imaging of pulmonary parenchyma using pulsed arterial spin labeling techniques: FAIRER and FAIR. J Magn Reson Imaging. 1999; 9:483–7. DOI: 10.1002/(SICI)1522-2586(199903)9:3<483::AID-JMRI18>3.0.CO;2-# [PubMed: 10194721]

14. Mugler JP, Altes TA. Hyperpolarized 129Xe MRI of the human lung. J Magn Reson Imaging. 2013; 37:313–31. DOI: 10.1002/jmri.23844 [PubMed: 23355432]

15. Wielpütz MO, Puderbach M, Kopp-Schneider A, Stahl M, Fritzsching E, Sommerburg O, et al. Magnetic Resonance Imaging Detects Changes in Structure and Perfusion, and Response to Therapy in Early Cystic Fibrosis Lung Disease. Am J Respir Crit Care Med. 2014; :1–49. DOI: 10.1164/rccm.201309-1659OC

16. Miller GW, Mugler JP, Sá RC, Altes Ta, Prisk GK, Hopkins SR. Advances in functional and structural imaging of the human lung using proton MRI. NMR Biomed. 2014; doi: 10.1002/nbm.3156

17. Dasenbrook EC, Lu L, Donnola S, Weaver DE, Gulani V, Jakob PM, et al. Normalized T1 magnetic resonance imaging for assessment of regional lung function in adult cystic fibrosis patients--a cross-sectional study. PLoS One. 2013; 8:e73286.doi: 10.1371/journal.pone.0073286 [PubMed: 24086277]

18. Altes TA, Eichinger M, Puderbach M. Magnetic resonance imaging of the lung in cystic fibrosis. Proc Am Thorac Soc. 2007; 4:321–7. DOI: 10.1513/pats.200611-181HT [PubMed: 17652494]

19. Kirby M, Svenningsen S, Ahmed H, Wheatley A, Etemad-Rezai R, Paterson NAM, et al. Quantitative Evaluation of Hyperpolarized Helium-3 Magnetic Resonance Imaging of Lung

Function Variability in Cystic Fibrosis. Acad Radiol. 2011; 18:1006–13. DOI: 10.1016/j.acra.2011.03.005 [PubMed: 21536462]

20. Eichinger M, Puderbach M, Fink C, Gahr J, Ley S, Plathow C, et al. Contrast-enhanced 3D MRI of lung perfusion in children with cystic fibrosis--initial results. Eur Radiol. 2006; 16:2147–52. DOI: 10.1007/s00330-006-0257-7 [PubMed: 16673092]
21. Fain SB, Korosec FR, Holmes JH, O'Halloran R, Sorkness RL, Grist TM. Functional lung imaging using hyperpolarized gas MRI. J Magn Reson Imaging. 2007; 25:910–23. DOI: 10.1002/jmri.20876 [PubMed: 17410561]
22. Bannier E, Cieslar K, Mosbah K, Aubert F, Duboeuf F, Salhi Z, et al. Hyperpolarized 3He MR for sensitive imaging of ventilation function and treatment efficiency in young cystic fibrosis patients with normal lung function. Radiology. 2010; 255:225–32. DOI: 10.1148/radiol.09090039 [PubMed: 20308459]
23. Gao Y, Goodnough CL, Erokwu BO, Farr GW, Darrah R, Lu L, et al. Arterial spin labeling-fast imaging with steady-state free precession (ASL-FISP): A rapid and quantitative perfusion technique for high-field MRI. NMR Biomed. 2014; 27:996–1004. DOI: 10.1002/nbm.3143 [PubMed: 24891124]
24. Kim SG, Tsekos NV. Perfusion imaging by a flow-sensitive alternating inversion recovery (FAIR) technique: application to functional brain imaging. Magn Reson Med. 1997; 37:425–35. [PubMed: 9055234]
25. Kwong KK, Chesler DA, Weisskoff RM, Donahue KM, Davis TL, Ostergaard L, et al. MR perfusion studies with T1-weighted echo planar imaging. Magn Reson Med. 1995; 34:878–87. [PubMed: 8598815]
26. Molinari F, Eichinger M, Risse F, Plathow C, Puderbach M, Ley S, et al. Navigator-triggered oxygen-enhanced MRI with simultaneous cardiac and respiratory synchronization for the assessment of interstitial lung disease. J Magn Reson Imaging. 2007; 26:1523–9. DOI: 10.1002/jmri.21043 [PubMed: 17968900]
27. Bolar DS, Levin DL, Hopkins SR, Frank LF, Liu TT, Wong EG, et al. Quantification of regional pulmonary blood flow using ASL-FAIRER. Magn Reson Med. 2006; 55:1308–17. DOI: 10.1002/mrm.20891 [PubMed: 16680681]
28. Jakob PM, Hillenbrand CM, Wang T, Schultz G, Hahn D, Haase A. Rapid quantitative lung 1H T1 mapping. J Magn Reson Imaging. 2001; 14:795–9. DOI: 10.1002/jmri.10024 [PubMed: 11747038]
29. Belle V, Kahler E, Waller C, Rommel E, Voll S, Hiller KH, et al. In vivo quantitative mapping of cardiac perfusion in rats using a noninvasive MR spin-labeling method. J Magn Reson Imaging. 8:1240–5. [PubMed: 9848735]

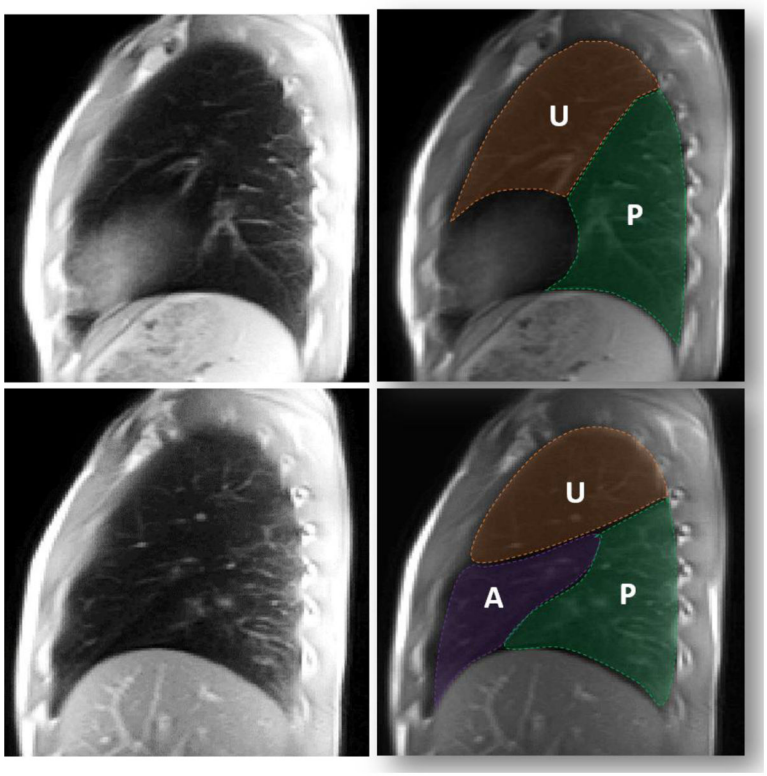

Figure 1.

Lung Region-of-Interest (ROI) Selection. Top row: Representative sagittal MRI image of the left lung of a healthy volunteer and the same image with overlaid ROI's delineating the two lobes (Upper = U, Posterior = P). Bottom row: Similar sagittal MRI images and corresponding ROI's for the right lung of a healthy volunteer (Upper = U, Anterior = A, Posterior = P).

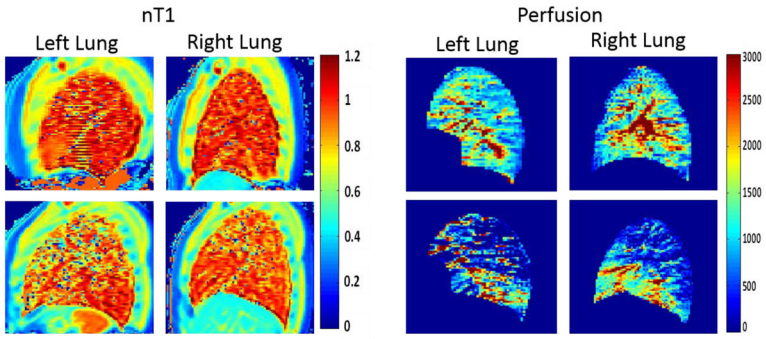

Figure 2.

Representative normalized T1 and perfusion maps for the left and right lungs of a healthy volunteer (top row) and a CF patient (bottom row). The maps for the subjects with CF show regions of visible decreases in normalized T1 and pulmonary perfusion (in ml/min/100g of tissue).

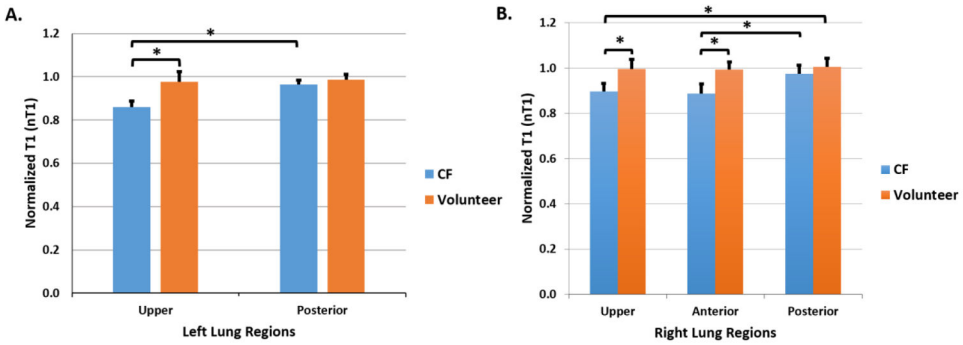

Figure 3.

Lobe-by-lobe analysis of normalized T1 (nT1) MRI Results. Mean nT1 values for A) the left lung regions (2 lobes); and B) right lung regions (3 lobes) for both the CF cohort (in blue, n = 8) and the healthy volunteers (in orange, n = 6). The CF cohort exhibited significant decreases in nT1 in the upper lobe of the left lung ($p = 0.00008$) as well as in the upper ($p = 0.0009$) and anterior lobes ($p = 0.0002$) of the right lung in comparison to healthy control subjects. Similar reductions in nT1 were observed in the upper and anterior lung regions of the left and right lungs within the CF cohort (left upper, $p = 0.0002$; right upper, $p = 0.0006$; right anterior, $p = 0.0005$) in comparison to the respective posterior lobes.

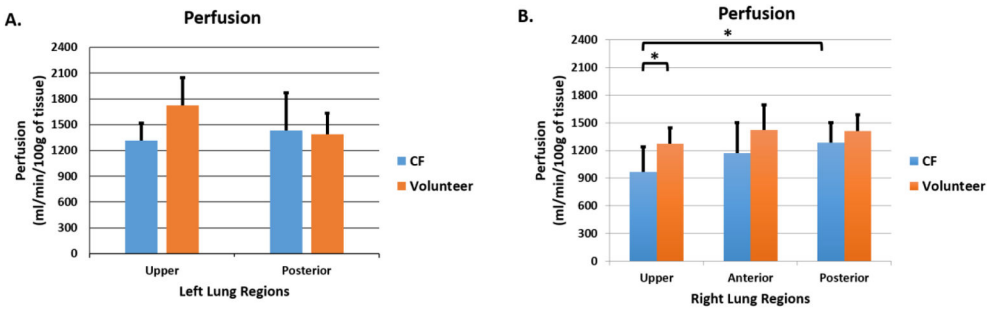

Figure 4.

Lobe-by-lobe analysis of ASL-based perfusion MRI Results. Mean pulmonary values for A) the left lung regions (2 lobes); and B) right lung regions (3 lobes) for both the CF cohort (in blue, n=8) and the healthy volunteers (in orange, n=6). The CF cohort exhibited no significant reduction in the left lung ($p > 0.1$). In the right lung, the mean pulmonary perfusion in upper lobe of the CF patients was significantly reduced in comparison to the upper lobe of healthy volunteers ($p = 0.02$) as well as in comparison to the posterior lobe of CF patients ($p = 0.02$).

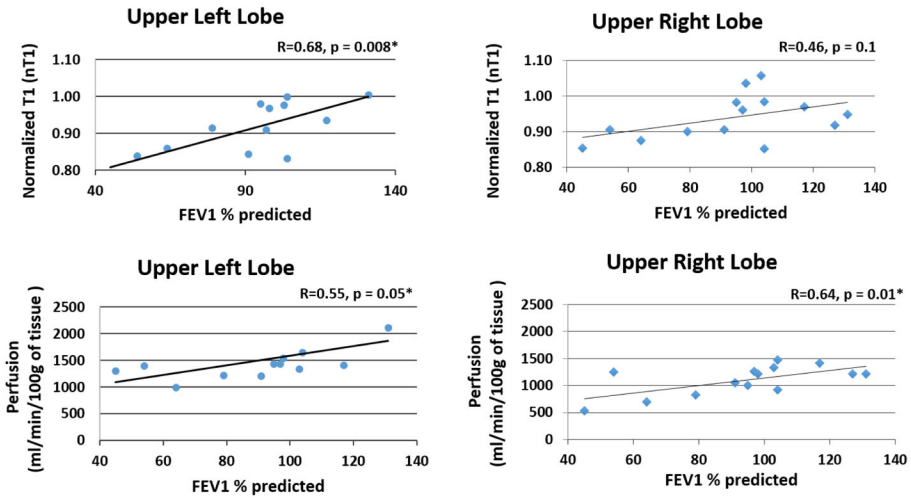

Figure 5.

Scatterplots of normalized T1 (top row) and pulmonary perfusion (bottom row) in the upper lobes of the left and right lungs for all subjects (CF patients and healthy volunteers) as a function of spirometry (FEV1 % predicted). Linear regression lines and Pearson Correlation coefficients are shown in each plot. Significant correlations were observed between nT1 and perfusion in the upper left lung regions. Only perfusion correlated significantly with lung function in the upper lobe of the right lung.

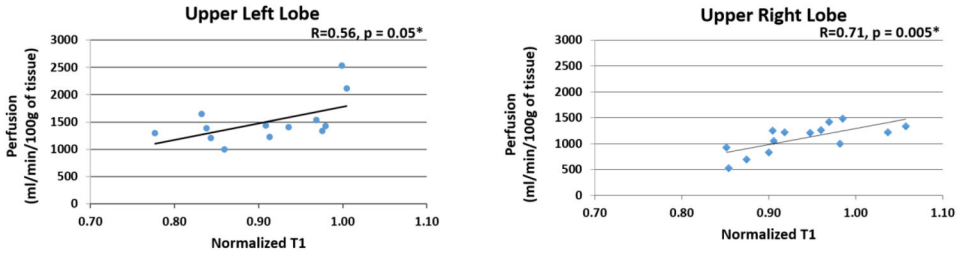

Figure 6.

Scatterplots of normalized T1 vs. perfusion in the upper lobes of the left and right lungs for the CF patients and healthy volunteers. A linear regression line and Pearson Correlation coefficient are shown for each plot. Significant correlations were observed for both the left ($p = 0.05$) and right lungs ($p=0.005$). No other lobes showed a significant correlation between the two MRI metrics